

PAPER • OPEN ACCESS

Adsorption of Cu^{2+} and rhodamine B by zeolite obtained from electrolytic manganese residue

To cite this article: C X Li *et al* 2020 *IOP Conf. Ser.: Earth Environ. Sci.* **612** 012038

View the [article online](#) for updates and enhancements.

You may also like

- [Laser induced fluorescence resonance energy transfer for detection of arsenic in water](#)
Simanta Hazarika and Chiranjib Rajkonwar
- [Degradation of dyes using reactive species of atmospheric pressure dielectric barrier discharge formed by a pencil plasma jet](#)
Vikas Rathore, Akanksha Pandey, Shruti Patel *et al.*
- [Synthesis of praseodymium-and molybdenum- sulfide nanoparticles for dye-photodegradation and near-infrared deep-tissue imaging](#)
Ye Wu, Pengfei Ou, Jun Song *et al.*



ECS
The
Electrochemical
Society
Advancing solid state &
electrochemical science & technology

DISCOVER
how sustainability
intersects with
electrochemistry & solid
state science research

Adsorption of Cu^{2+} and rhodamine B by zeolite obtained from electrolytic manganese residue

C X Li^{1,2}, Y Yu¹ and Q W Zhang¹

¹College of Safety Science and Engineering, Nanjing Tech University, Nanjing 211816, Jiangsu, China

²E-mails: lichangxin2010@njtech.edu.cn / lichangxin20160706@163.com

Abstract. The adsorption of Cu^{2+} and rhodamine B from aqueous solutions onto zeolite derived from electrolytic manganese residue (EMR) via a fusion method was investigated. The adsorption kinetic for Cu^{2+} and rhodamine B onto EMR-based zeolite (EMRZ) was explored and best determined by Pseudo-second-order kinetic model. And the adsorption capacity of Cu^{2+} and rhodamine B reach up to 66.86 and 18.96 $\text{mg}\cdot\text{g}^{-1}$ respectively.

1. Introduction

As Cu^{2+} and rhodamine B are the relatively common pollutants in water, Cu^{2+} and rhodamine B were used to assess the adsorption capability of zeolite derived from electrolytic manganese residue. Rhodamine B and Cu^{2+} in wastewater can be purified in many ways, such as coagulation, adsorption, and chemical oxidation. In the known process, adsorption taking zeolite as adsorbent has been recognized as a valid and competitive treatment way due to its cost performance and simple operation [1-5]. Moreover, the open and stable three-dimensional honeycomb structure of zeolites making them possess high cation exchange capacity (CEC) and strong adsorption for rhodamine B and Cu^{2+} [6,7].

Electrolytic manganese residue (EMR) is mainly generated during the acid reduction stage for manganese ore in the electrolytic metal manganese (EMM) industry. Currently, almost all of the EMR is piled up into storage points around the EMM factory without any treatment. With long-term accumulation, pollutants, such as heavy metals in EMR can gradually penetrate into the environment, posing great risk for the local ecology environment. On the other hand, a large amount of accumulation of EMR will also bring huge economic pressure to EMM production company owing to routine maintenance and new stockpiling site costs. Therefore, it is very important to research advanced technology for the efficient utilization of EMR. Lately, our research team found that EMR can be used to fabricate zeolite, which can be served as an environment friendly application of EMR.

The main purpose of this research is to probe the feasibility of using EMR-based zeolite (EMRZ) to absorb Cu^{2+} and rhodamine B ions from aqueous solutions. Moreover, the adsorption kinetics for Cu^{2+} and rhodamine B onto EMRZ were also systematically discussed.

2. Materials and Methods

2.1. Materials

The EMR adopted in this research was obtained from an EMM enterprise located in west of Hunan, China. The chemical composition of EMR was analyzed and displayed as follows: $\text{Na}_2\text{O}=2.7\text{wt}\%$, $\text{SiO}_2=24.6\text{wt}\%$, $\text{Al}_2\text{O}_3=12.2\text{wt}\%$, $\text{MgO}=1.7\text{wt}\%$, $\text{K}_2\text{O}=2.4\text{wt}\%$, $\text{CaO}=8.6\text{wt}\%$, $\text{MnO}=4.6\text{wt}\%$ and



$\text{Fe}_2\text{O}_3=7.9\text{wt}\%$. The EMRZ was manufactured of taking EMR as raw material via a fusion method. And the detailed preparation and characterization methods were both described in our previous related studies [8]. All chemicals employed in the experiment, such as $\text{Cu}(\text{NO}_3)_2$ and rhodamine B ($\text{C}_{28}\text{H}_{31}\text{N}_2\text{O}_3\text{Cl}$) are analytically pure and purchased from Sinopharm Chemical Reagent Co., Ltd.

2.2. Adsorption studies

For a typical adsorption process, 0.3 g of EMRZ was firstly mixed into an Erlenmeyer flask (250 mL) having 100 mL of $300\text{mg}\cdot\text{L}^{-1}$ of Cu^{2+} and rhodamine B solution at pH 6.0. Then, the flask was placed in an oscillator at 30°C and oscillated at 200 rpm for a given time. At the designated time, the suspension was taken out and filtered by filter paper and the concentrations of Cu^{2+} and rhodamine B in the filtrate were analyzed respectively. The Cu^{2+} and rhodamine B adsorbed on EMRZ were evaluated and calculated by following formula.

$$q_e=(C_0-C_e)V/m \quad (1)$$

where C_0 and C_e are the concentrations of Cu^{2+} and rhodamine B (mg/L) obtained at initial and equilibrium time, q_e (mg/g) is the adsorption capacity for Cu^{2+} and rhodamine B onto EMRZ, V is the volume of aqueous solution applied in the adsorption process (L), and m is the mass of EMRZ used in the adsorption process (g).

2.3. Characterization

XRD (D8 Discover, Bruker, Germany), XRF (Axios, PANalytical, Holland) and FE-SEM (Mira3, Tescan, Czech Republic) were employed to investigate the mineralogy, chemical composition and morphological structure of EMRZ, respectively. BET equation by N_2 adsorption method on ASAP2020 (Micromeritics, USA) was employed to evaluate the SSA (specific surface area). And the CEC value of EMRZ was assessed via the method of Zhang et al. [9]. The Cu^{2+} ions concentration was analyzed by atomic absorption spectrophotometers (Thermo Electron, USA). And rhodamine B concentration was analyzed by Shimadzu UV-visible spectrophotometer at 555nm.

3. Results and Discussion

3.1. Characterization of EMRZ

From Figure 1, zeolite A and zeolite P were both detected in the EMRZ, and zeolite A was the main phase composition. Moreover, the coexist of zeolite A (cubes crystals) and zeolite P (round crystals) in the EMRZ was also proved by FE-SEM (see Figure 2). The obtained EMRZ with $\text{Si}/\text{Al}=1.01$ was synthesized from EMR. And, the low Si/Al ratio of EMRZ was attribute to generation of zeolite A and P. Meanwhile, the CEC and SSA values were 3.45 meq/g and $39.38\text{ m}^2/\text{g}$, respectively. And the CEC value for the obtained EMRZ (i.e. 3.45 meq/g) is obviously higher than those prepared from related waste [8,10,11], which implies the possibility of using EMRZ as an adsorbent for adsorption.

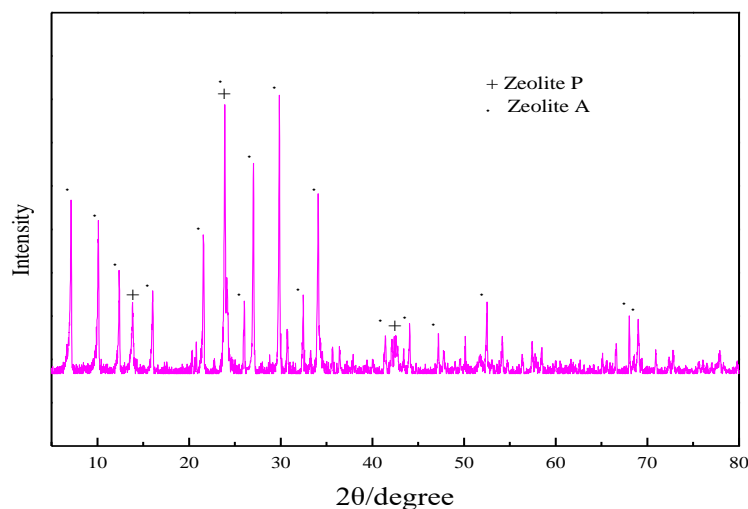


Figure 1. The XRD pattern of EMRZ.

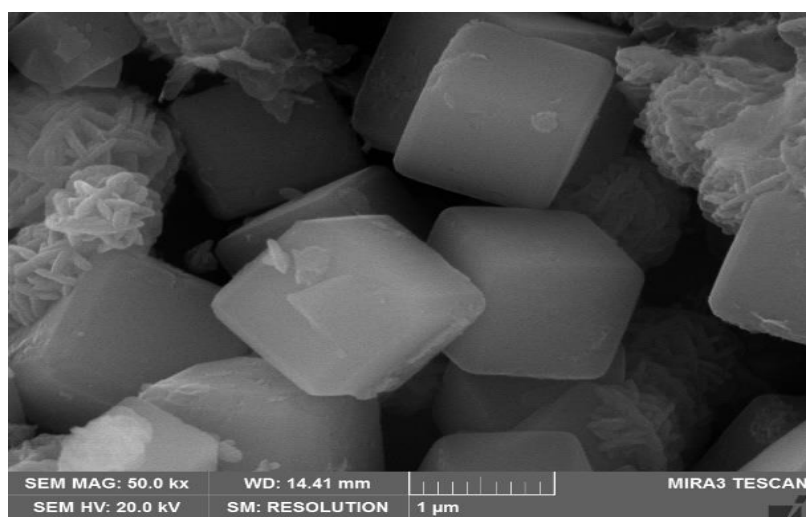


Figure 2. FE-SEM images of EMRZ.

3.2. Adsorption properties of EMRZ

The removal of Cu^{2+} and rhodamine B onto EMRZ was examined to evaluate the adsorption properties of EMRZ. And the results for the removal of Cu^{2+} and rhodamine B are listed in Figure 3. From Figure 3, Cu^{2+} adsorption process onto EMRZ progressed rapidly within the first 210 minutes, and then slowly tended to adsorption equilibrium. The above behavior could be attribute to the reason that all the adsorption sites are empty at the beginning and the increasing driving force generated from high solute concentration gradient is inevitable [12,13]. Meanwhile, a similar adsorption process was also obtained in the adsorption of rhodamine B. Meanwhile, as seen from Figure 3, Cu^{2+} adsorption onto EMRZ was higher than rhodamine B. Since Cu^{2+} has lower radius than that of rhodamine B, the diffusion for Cu^{2+} was faster and rhodamine B was retarded when the dye moved through the pores during the adsorption process. This difference causes Cu^{2+} to be attracted to the EMRZ surface stronger than Rhodamine B. And a possible mechanism for rhodamine B removal onto EMRZ is the interaction between the hydroxyl group in EMRZ and the cation in rhodamine B.

The kinetic models including Pseudo-first-order and Pseudo-second-order kinetic models were both taken to determine the best fit model by implementing them on resultant data to clarify the adsorption

process. The Pseudo-first-order and Pseudo-second-order kinetic models are identified with below formula [14-16]:

$$\ln(q_e - q_t) = \ln q_e - k_1 t \quad (2)$$

$$\frac{t}{q_t} = \frac{1}{k_2 q_e^2} + \frac{t}{q_e} \quad (3)$$

where q_e and q_t are the adsorption capacity for Cu^{2+} and rhodamine B onto EMRZ ($\text{mg} \cdot \text{g}^{-1}$) at equilibrium and at time t . k_1 (min^{-1}) and k_2 ($\text{g} \cdot \text{mg}^{-1} \cdot \text{min}^{-1}$) are the adsorption constants.

The model constants were obtained by the above models and were shown in Table 1 and Figure 4. Seen from Table 1, correlation coefficients ($R^2=0.9869$ for Cu^{2+} and $R^2=0.9774$ for rhodamine B) obtained by Pseudo-second-order model are much higher than the correlation coefficients ($R^2=0.7530$ for Cu^{2+} and $R^2=0.7460$ for rhodamine B) obtained by Pseudo-first-order model. Moreover, the value of q_e (theoretical adsorption capacity) calculated by the Pseudo second-order model is closer to the value of $q_e(\text{exp})$ (experimental adsorption capacity). Therefore, the above data shows that the adsorption process of Cu^{2+} and rhodamine B is more suitable with the pseudo-second-order model.

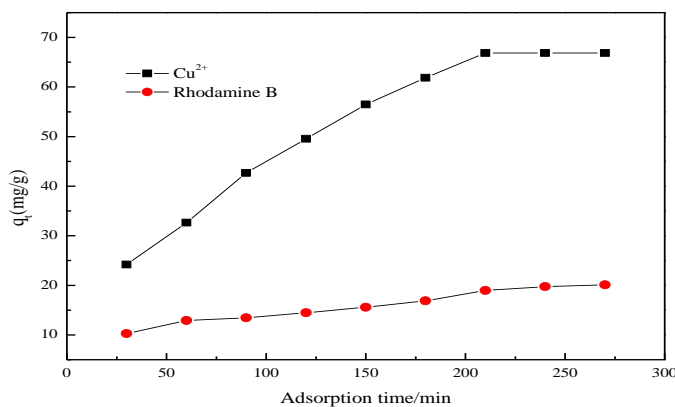


Figure 3. Effect of contact time on Cu^{2+} and rhodamine B adsorption (initial concentration= $300 \text{ mg} \cdot \text{L}^{-1}$; EMRZ dose= $0.3 \text{ g}/100\text{mL}$; pH value= 6.0 ; temperature = $30 \text{ }^\circ\text{C}$).

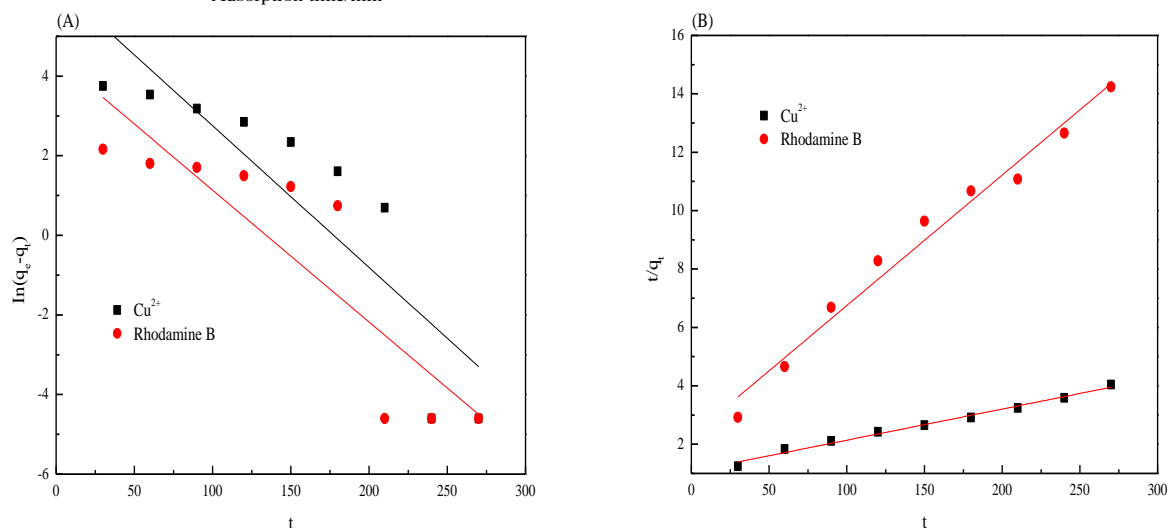


Figure 4. (A) Pseudo-first order, and (B) Pseudo-second-order model kinetic plots for Cu^{2+} and rhodamine B adsorption onto EMRZ (initial concentration= $300 \text{ mg} \cdot \text{L}^{-1}$; EMRZ dose= $0.3 \text{ g}/100\text{mL}$; pH value= 6.0 ; temperature= $30 \text{ }^\circ\text{C}$).

Table 1. Kinetic parameters for Cu²⁺ and rhodamine B removal.

Adsorbate	q _e (exp) /mg·g ⁻¹	pseudo-first-order model			pseudo-second-order model		
		q _e (mg·g ⁻¹)	k ₁ (min ⁻¹)	R ²	q _e (mg·g ⁻¹)	k ₂ (g·mg ⁻¹ · min ⁻¹)	R ²
Cu ²⁺	66.86	551.32	0.0365	0.7530	93.81	1.0604×10 ⁻⁴	0.9869
rhodamine B	18.96	85.91	0.03315	0.7460	22.38	8.7599×10 ⁻⁴	0.9774

4. Conclusions

EMR-based zeolite (EMRZ) can be successfully prepared from EMR via a fusion method. And zeolite A and zeolite P were both detected in the EMRZ, and zeolite A was the main phase composition. And adsorption of Cu²⁺ and rhodamine B onto EMRZ can be accomplished in an efficient and suitable process. The adsorption process of Cu²⁺ and rhodamine B is more suitable with the Pseudo-second-order model. This research develops new idea and novel adsorbent for the adsorption of Cu²⁺ and rhodamine B.

Acknowledgements

This work was financially supported by China Postdoctoral Science Foundation (No. 2017M611799) and Jiangsu Provincial Basic Research Program (Natural Science Foundation) (No. BK20190690).

References

- [1] Sprynskyy M, Lebedynets M, Terzyk A P, Kowalczy P, Namieśnik J and Buszewski B 2005 Ammonium sorption from aqueous solutions by the natural zeolite Transcarpathian clinoptilolite studied under dynamic conditions *J. Colloid Interface Sci.* **284** 408-15
- [2] Marañón E, Ulmanu M, Fernández Y, Anger I and Castrillón L 2006 Removal of ammonium from aqueous solutions with volcanic tuff *J. Hazard. Mater.* **B137** 1402-9
- [3] Jain R, Mathur M, Sikarwar S and Mittal A 2007 Removal of the hazardous dye rhodamine B through photocatalytic and adsorption treatments *J. Environ. Manage.* **85** 956-64
- [4] Gupta V K, Ali I and Saini V K 2004 Removal of rhodamine B, fast green, and methylene blue from wastewater using red mud, an aluminum industry waste *Ind. Eng. Chem. Res.* **43** 1740
- [5] Gad H M H and El-Sayed A A 2009 Activated carbon from agricultural by-products for the removal of rhodamine-B from aqueous solution *J. Hazard. Mater.* **168** 1070-81
- [6] Nguyen M L and Tanner C C 1998 Ammonium removal from wastewaters using natural New Zealand zeolites *N. Z. J. Agric. Res.* **41** 427-46
- [7] Lebedynets M, Sprynskyy M, Sakhnyuk I, Zbytniewski R, Golembiewski R and Buszewski B 2004 Adsorption of ammonium ions onto a natural zeolite: transcarpathian clinoptilolite *Adsorpt. Sci. Technol.* **22** 731-41
- [8] Li C X, Zhong H, Wang S, Xue J R and Zhang Z Y 2015 Removal of basic dye (methylene blue) from aqueous solution using zeolite synthesized from electrolytic manganese residue *J. Ind. Eng. Chem.* **23** 344-52
- [9] Zhang M, Zhang H, Xu D, Han L, Niu D X, Tian B H, Zhang J, Zhang L Y and Wu W S 2011 Removal of ammonium from aqueous solutions using zeolite synthesized from fly ash by a fusion method *Desalination* **271** 111-21
- [10] Milan Z, Sanchez E, Weiland P, de Las Pozas C, Borja R, Mayari R and Rovirosa N 1997 Ammonia removal from anaerobically treated piggery manure by ion exchange in columns packed with homoionic zeolite *Chem. Eng. J.* **66** 65-71
- [11] Booker N A, Cooney E L and Priestly A J 1996 Ammonia removal from sewage using natural Australian zeolite *Water Sci. Technol.* **34** 17-24
- [12] Khan T A, Dahiya S, Ali I 2012 Use of kaolinite as adsorbent: equilibrium, dynamics and thermodynamic studies on the adsorption of rhodamine B from aqueous solution *Appl. Clay. Sci.* **69** 58-66

- [13] Gusain D, Srivastava V and Sharma Y C 2014 Kinetic and thermodynamic studies on the removal of Cu (II) ions from aqueous solutions by adsorption on modified sand *J. Ind. Eng. Chem.* **20** 841-7
- [14] Cheng Y C, Huang T L, Shi X X, Wen G and Sun Y K 2017 Removal of ammonium ion from water by Na-rich birnessite: performance and mechanisms *J. Environ. Sci.* **57** 402-10
- [15] He Y H, Lin H, Dong Y B, Liu Q L and Wang L 2016 Simultaneous removal of ammonium and phosphate by alkaline-activated and lanthanum-impregnated zeolite *Chemosphere* **164** 387-95
- [16] Widiastuti N, Wu H W, Ang H M and Zhang D K 2011 Removal of ammonium from greywater using natural zeolite *Desalination* **277** 15-23